

Self-Assembly of Gold Nanowires along Carbon Nanotubes for Ultrahigh-Aspect-Ratio Hybrids

Wenrong Yang,^{*,†,‡} Liangti Qu,[§] Rongkun Zheng,[†] Zongwen Liu,[†] Kyle R. Ratinac,[†] Luming Shen,[⊥] Dingshan Yu,[§] Lin Yang,^{||} Colin J. Barrow,[‡] Simon P. Ringer,[†] Liming Dai,^{*,§} and Filip Braet[†]

[†]Australian Centre for Microscopy & Microanalysis, The University of Sydney, Sydney, New South Wales 2006, Australia

[‡]School of Life and Environmental Sciences, Deakin University, Waurn Ponds, Victoria 3217, Australia

[§]Department of Chemical Engineering, Case School of Engineering, Case Western Reserve University, 10900 Euclid Avenue, Cleveland, Ohio 44106, United States

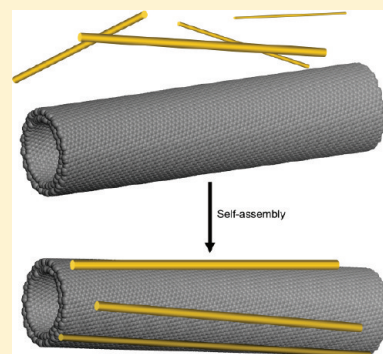
[⊥]School of Civil Engineering, The University of Sydney, Sydney, New South Wales 2006, Australia

^{||}Cyrus Tang Hematology Center, Soochow University, Suzhou, Jiangsu, People's Republic of China

S Supporting Information

ABSTRACT: We report a novel approach for the assembly of one-dimensional hybrid nanostructures that consist of gold nanowires with ultrahigh aspect ratios ($L/d > 500$) self-assembled along the axes of multiwalled carbon nanotubes. The micrometer-long hybrid nanowires exhibit high electrical conductivity and can be easily microcontact-printed onto various substrates in a patterned form, suggesting that these hybrids have considerable potential as interconnects for nanoelectronic applications.

KEYWORDS: nanostructures, nanotubes, hybrids, self-assembly



INTRODUCTION

The ability to control the synthesis and self-assembly of nanostructures with ultrahigh aspect ratios will play an important role in the design of next-generation optoelectronic devices^{1–8} and other nanotechnologies. These nanoscale materials will form the building blocks of multifunctional devices that, when fabricated through precise control of the chemical and surface forces, will allow us to overcome the fundamental and economic limitations of conventional lithography-based (or “top-down”) fabrication.^{3,9,10} With their ultrahigh aspect ratios, long nanowires provide new opportunities for self-assembly as well as for the transfer of electronic, optical, thermal, or other signals over large length scales.

During the past decade, considerable progress has been made in the synthesis of hybrid nanostructures, such as carbon nanotube (CNT)—inorganic hybrids, by various wet-chemistry methods.¹¹ For instance, gold (Au) nanorods ($L/d \sim 2.5$, where $L \sim 30$ nm) functionalized with anionic poly(vinylpyrrolidone) have been electrostatically assembled on the surface of cationic poly(diallyldimethylammonium chloride)-coated CNTs.¹² This assembly process exploited the low surface potentials of the nanorods’ ends, compared with their sides, to encourage end-to-end assembly of the nanorods along the lengths of the nanotubes. Despite such efforts, however, it remains challenging to assemble hybrid nanomaterials with large aspect ratios (e.g., diameters smaller than 10 nm

and lengths of micrometers or more, as in the present study) in a controlled and efficient way.^{13,14}

The recent report of facile methods for the preparation of ultrathin Au nanowires^{1,15–24} has prompted us to undertake the present study, in which we have developed a simple and rapid method for the self-assembly of Au nanowires along CNTs. The driving force of our self-assembly process is the strong van der Waals and hydrophobic interactions that occur between the side chains of oleylamine-coated Au nanowires and the sidewalls of CNTs. These surface forces allow the assembly of one-dimensional hybrid structures, comprising ultralong Au nanowires adsorbed along the length of CNTs, without the prerequisite for functionalization of nanotube surfaces (Figure 1). Furthermore, we have also demonstrated that these micrometer-long hybrid nanowires can be easily microcontact-printed (μ CP) onto various substrates in a patterned form. Therefore, this approach is potentially useful for organizing novel one-dimensional nanostructures as building blocks for the bottom-up assembly of new electronic and photonic nanosystems.²⁵

EXPERIMENTAL SECTION

All chemicals and solvents were purchased from Sigma-Aldrich and used without further purification.

Received: November 28, 2010

Revised: March 29, 2011

Published: May 04, 2011

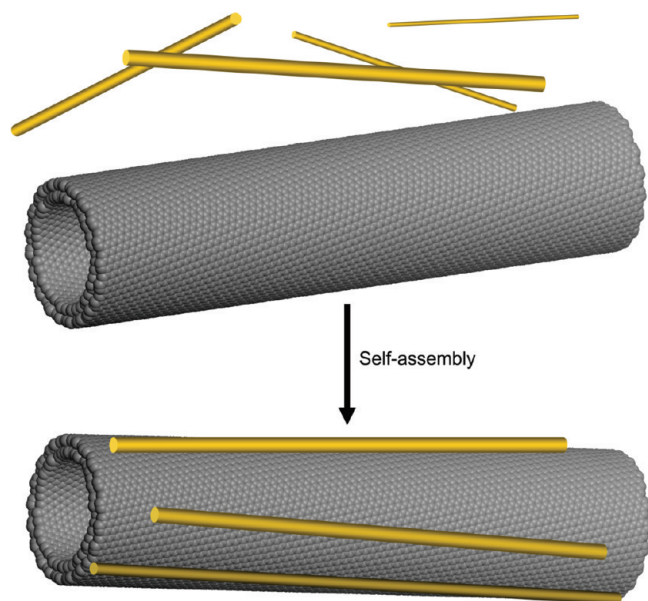


Figure 1. General scheme of Au nanowire self-assembly onto CNTs. The interaction between nanowires and MWNTs leads to the formation of hybrid nanostructures.

Synthesis of Hybrid Nanostructures. The ultrathin single-crystal Au nanowires used in this study were synthesized according to the method developed by Yang's group.¹⁷ The reaction typically produces uniform, continuous, and ultrathin nanowires dispersed in a purple solution. Because some Au nanoparticles often form in addition to the nanowires, we filtered the solution through a hydrophobic Durapore 0.22 μm membrane to remove the nanoparticles. The final product was then washed several times with a toluene and ethanol mixture (1:3, v/v) to remove excess oleylamine. The as-prepared Au nanowires, coated with oleylamine, are hydrophobic and can be dispersed readily in hexane. They are also highly flexible: the nanowires, once dried on a transmission electron microscopy (TEM) grid, were frequently observed to be looped or bent (see Figure S1 in the Supporting Information). To produce the hybrid material, we combined the as-prepared Au nanowires in hexane with a dispersion of multiwalled nanotubes (MWNTs) in hexane; each solution had a concentration of up to 0.2 mg/mL. Mixtures were gently shaken for 20 min to enhance the interaction between the MWNTs and the polar heads of the oleylamine molecules covering the nanowires.

Characterization of Hybrid Nanostructures. To characterize the nanostructure of the hybrids, a 10 μL drop of the mixed solution was deposited on a carbon-coated copper TEM grid and dried for 1 h before examination in a scanning transmission electron microscope (STEM; VG HB601 system) operated at an accelerating voltage of 100 kV. Besides conventional bright-field (BF) imaging in the STEM, we also used high-angle annular dark-field (HAADF) imaging in the STEM to obtain atomic number contrast (or "Z-contrast") micrographs of the hybrids.

Molecular Dynamics (MD) Simulation of the Self-Assembly of Au Nanowires and MWNTs. The MD simulation modeled the interaction between (30, 30), (35, 35), (40, 40) MWNTs, with a length of 36.77 nm, and an Au nanowire, with dimensions of 1.63 nm \times 1.63 nm \times 36.77 nm, by using the MD code LAMMPS²⁶ (<http://lammps.sandia.gov/>). The interatomic interactions were modeled with the embedded-atom method potential^{27,28} for the Au–Au interaction, Brenner's potential²⁹ for the C–C interaction, and a Lennard–Jones potential with parameters given in refs 30 and 31 for the Au–C interaction. In the beginning of the MD simulation, the MWNT and Au nanowire were inserted parallel to the center of the simulation

supercell. The size of the supercell was 45 nm \times 45 nm \times 36.77 nm, and the MWNT and nanowire were aligned along the direction of length 36.77 nm. The initial edge-to-edge distance between the MWNT and Au nanowire was about 0.82 nm. Periodic boundary conditions were enforced in all three directions. The system temperature was kept at 300 K using a Nose/Hoover temperature thermostat.³² The time (t) step was 1 fs in the simulation.

Pattern Formation with the Hybrids. Silicon slides were cleaned by immersion in a freshly prepared "piranha" solution [1:2 (v/v) H_2O_2 (30%)/ H_2SO_4 (96%)] for 1 h. **Warning!** *piranha solution reacts strongly with organic materials and should be handled with extreme caution.* The silicon substrates were then washed with deionized ultrafiltered water (Fisher) and dried in a stream of high-purity nitrogen. Microcontact printing, a soft-lithographic technique, was used to pattern thiol-group-enriched areas onto the glass surfaces. Each time, a poly(dimethylsiloxane) stamp was used to regiospecifically transfer a (3-mercaptopropyl)-trimethoxysilane (MPTMS) solution [1:2 (v/v) MPTMS/chloroform] onto the cleaned surface. The slides were then gently rinsed with chloroform and ultrafiltered deionized water and dried with nitrogen gas. A solution, of an appropriate concentration, of Au nanowires on CNTs in hexane was then dropped onto the patterned surface to allow chemical interactions between the Au nanowires and surface-bound thiol groups. The surfaces were then allowed to dry.

RESULTS AND DISCUSSION

Figure 2 presents STEM BF and HAADF micrographs of one of the as-prepared hybrid nanowires (parts a and b). The low-magnification image (Figure 2a) shows that the assembly is extremely uniform over a large portion of the nanotube length, while the higher magnification images (Figure 2c,d) show the alignment of Au nanowires along the CNT to form approximately longitudinal stripes. From high-resolution images (Figure 2e), we estimated the mean distance between the Au nanowires and the surface of the MWNT to be approximately 2 nm, close to the chain length ($X.Y$ nm) of the oleylamine chains that coat the nanowires. The HAADF images use a high-angle annular detector to form the image and so only collect electrons that have been Rutherford-scattered by the nuclei of the atoms in the sample. As a result, the brightness in HAADF images is not representative of the diffracted intensity, as is the case in conventional dark-field images, but rather of the nuclear charge (or atomic number, Z) of the atoms present. Consequently, the high brightness of the nanowires is as would be expected for the high Z of the Au nanowires, while the MWNTs show less contrast because they are made only of carbon.

We also examined the effect of the aspect ratio, from L/d of approximately 20 to 500, on the nature of the nanowire alignment along the nanotube axes. The Au nanowires with the highest aspect ratio, L/d of approximately 2000, tended to align along the sidewall of the MWNT with uniform coverage, as is evident from Figure 2a,b. Similar results were obtained for the assembly of nanowires with aspect ratios all the way down to L/d of about 80 (data not shown). This suggests that even moderate aspect ratios still provide sufficient surface area for the nanowires to allow their longitudinal adsorption on the MWNTs. Given this aligned arrangement, we have termed the hybrids "nanostripes".

To investigate the surface forces responsible for this controlled assembly, we also prepared hybrid samples in which the MWNTs were first covered with sodium dodecyl sulfate (SDS) to impart a polar character to the nanotube surfaces. In this case, a few Au nanowires assembled on these hydrophilic MWNTs (data not shown). This finding suggests that van der Waals

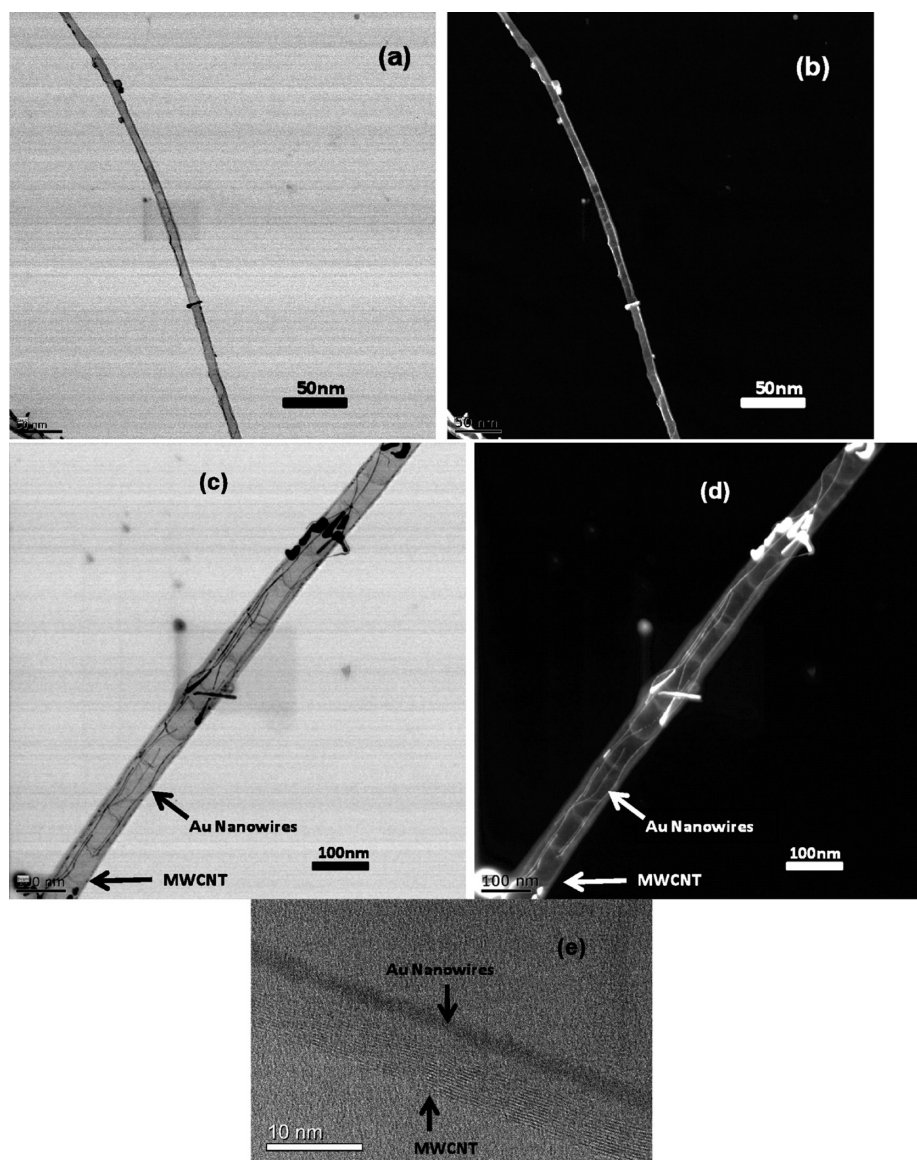


Figure 2. TEM micrographs showing the assembly of Au nanowires along a MWNT: (a) a BF image, in which the Au nanowires appear dark, and (b) the corresponding ADF image, which shows the Au nanowires in bright contrast; (c) a BF image and (d) an ADF image at higher magnification; (e) a high-resolution BF image showing an individual Au nanowire along the layered graphitic fringe of the CNT sidewall. Scale bars: (a) 50 nm; (b) 50 nm; (c) 100 nm; (d) 100 nm; (e) 10 nm.

and hydrophobic interactions between the oleylamine side chains of the Au nanowires and the sidewalls of unmodified CNTs are responsible for the successful assembly of hybrid nanostripes.

We performed preliminary MD simulations to further investigate the self-assembly of Au nanowires and MWNTs when in close proximity. The initial edge-to-edge distance between the MWNT and Au nanowire was set to 0.82 nm, and the top and side views of the MWNT and Au nanowire system at times, t , of 0, 3, 6, and 9 ps are presented in Figure 3 (which was produced with the software *VMD*³³). These preliminary results show that the MWNT and Au nanowire attract and attach to each other if they are close enough. It seems likely that this attraction is due to hydrophobic forces, and ubiquitous van der Waals forces, given that the introduction of the polar SDS molecules eliminated almost all interactions between the nanowires and nanotubes, as

is evidenced by the almost complete absence of adsorbed nanowires on SDS-coated MWNTs. Even if these forces were insufficient to attract the Au nanowires to the MWNTs because of the large initial separations (greater than 1 nm) in the solution, evaporation of the solvent would reduce these distances. Of course, capillary forces and surface tension during drying could be implicated in the self-assembly,³⁴ and also chemical interactions between nanoparticles,³⁵ although these forces depend on the solvent and any surfactant (e.g., SDS) in the solution, the substrate morphology, and the geometry of the nanoparticles.³⁶ In any case, these forces, although possibly reduced by the presence of surfactant molecules, would also have been present in the system containing the SDS adsorbed on the MWNTs. This suggests that hydrophobic forces dominated any effects due to the capillary forces and surface tension during drying of samples.

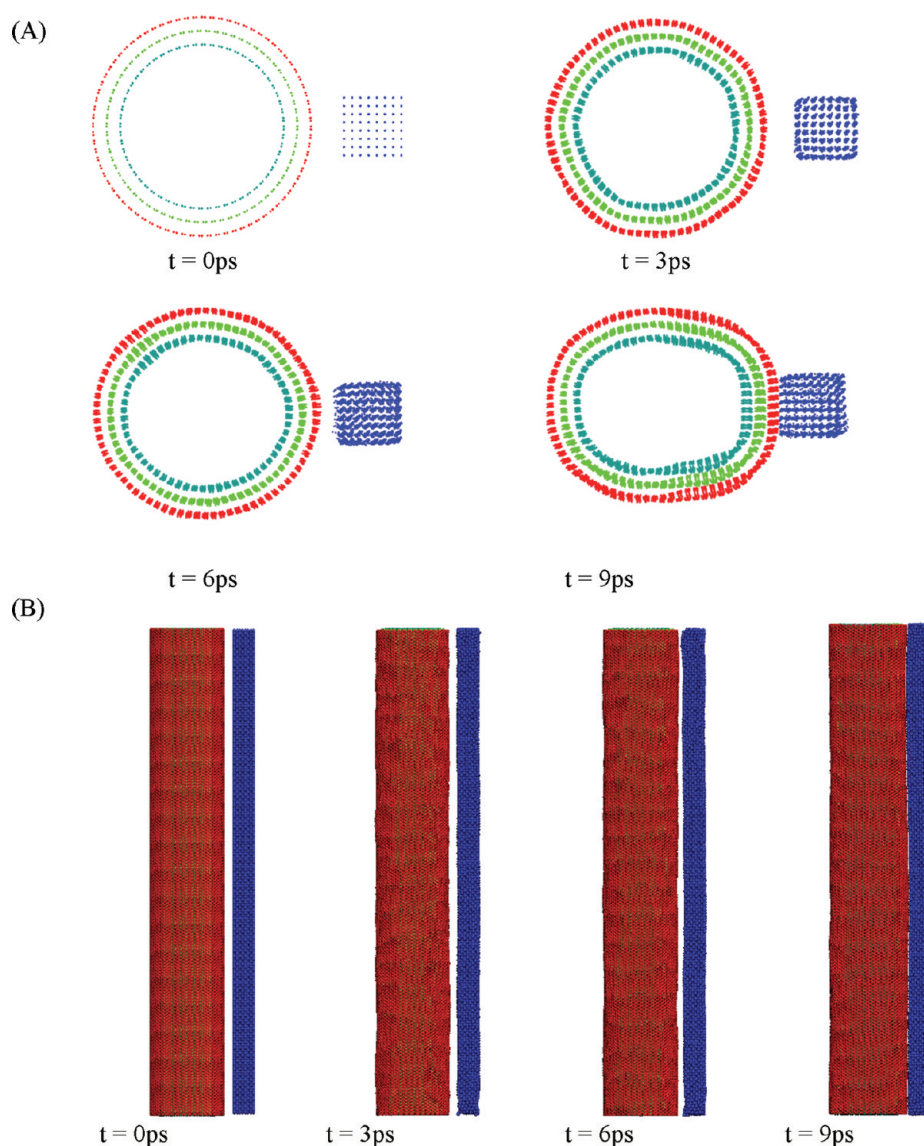


Figure 3. (A) Top views of the Au nanowire and MWNT system with an initial separation of 0.82 nm at different times. (B) Side views of the Au nanowire and MWNT system with an initial separation of 0.82 nm at different times.

To explore the potential use of the nanostripes, we used the soft-lithographic technique^{37,38} of microcontact printing to create a pattern of these hybrids [Figure 4A(a–c)]. In view of the large body of publications, including ours, in the literature about the use of μCP for uniform pattern formation,^{39–42} we used chemical adsorption between the Au nanowires and μCP patterned thiol for the formation of patterns of the Au nanowire/MWNT nanostripes on the silicon surface. The typical micropatterns of the nanostripes, as seen by scanning electron microscopy (SEM), are shown in Figure 4A(d). The patterns of one-dimensional hybrid nanostructures thus prepared have accurate spatial placement down to the submicrometer scale. Such a simple method for generating micropatterns of aligned nanostripes could open avenues for the fabrication of various multifunctional nanostructures for potential applications from novel stretchable electronic devices⁴³ to electromechanical systems.⁴⁴

To demonstrate the suitability of the nanostripes for such applications, we have also measured the electrical transport properties of the as-prepared hybrids deposited from their hexane

dispersion across two Au electrodes prefabricated on a SiO_2 -capped silicon surface.⁴⁵ For comparison, a similar device was fabricated with pure MWNTs under the same conditions. The electron-transport measurements show that the hybrid nanostripes can support a high current flow (Figure 4B). As can be seen, the resistance of the hybrid nanostripes is small compared to the MWNTs and to silicon nanowires (usually on the order of megaohms), suggesting that these hybrid nanostripes could be used as high-performance interconnects for nanoelectronic applications.⁴⁶ As hybrid nanostripes with ultrahigh aspect ratios, they may facilitate electrical transport as an efficient nanoscale assembly technique. The results suggest that these nanostripes could outperform for use as on-chip interconnects, tiny wires that are used to connect transistors and other devices on integrated circuits. Their use as interconnects could help extend the long run of performance improvements for silicon-based integrated circuit technology. We believe that there are potential advantages of using the hybrid nanostripes as future interconnects.⁴⁷

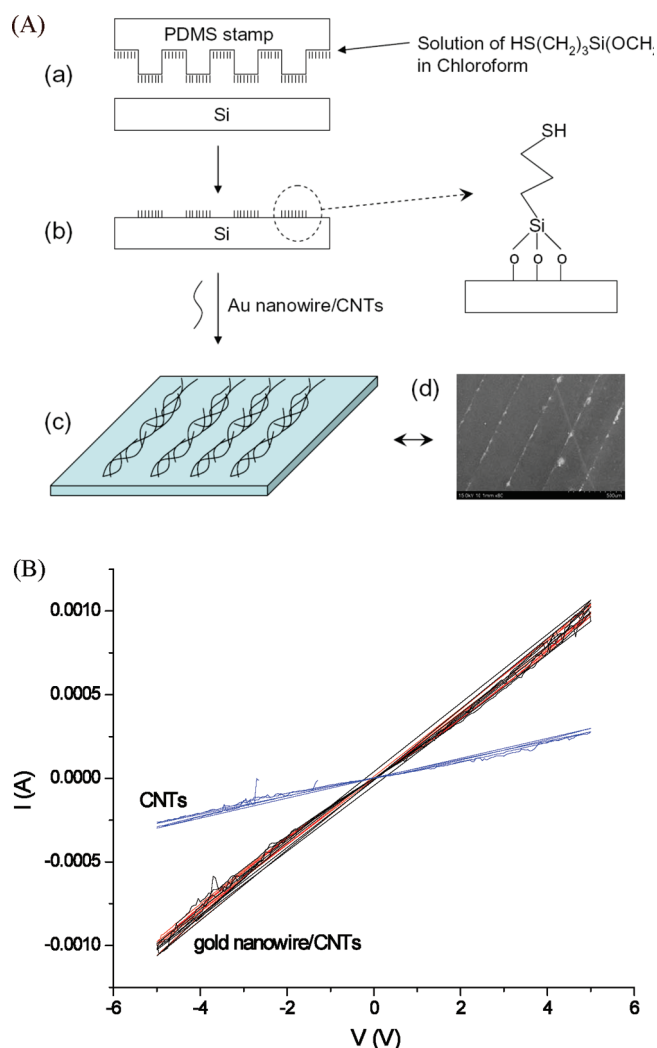


Figure 4. (A) Patterning of nanostructures by microcontact printing. (B) Comparison of the I - V response for nanostructures and MWNTs, showing the enhanced current flow through the hybrids.

CONCLUSION

In conclusion, we have presented a simple, but effective, method for the self-assembly of one-dimensional hybrid nanostructures from CNTs and ultrathin Au nanowires. We demonstrated that these micrometer-long hybrids can be easily patterned onto surfaces and display good electronic conductivity with a low resistance compared with pure MWNTs. This indicates that these hybrid nanostructures could conceivably be used as molecular-scale interconnects for future nanoscale electronics.

ASSOCIATED CONTENT

Supporting Information. TEM image of the Au nanowires. This material is available free of charge via the Internet at <http://pubs.acs.org>.

AUTHOR INFORMATION

Corresponding Author

*E-mail: wenrong.yang@sydney.edu.au (W.Y.), liming.dai@case.edu (L.D.).

ACKNOWLEDGMENT

The authors acknowledge the facilities as well as scientific and technical assistance from staff in the Australian Microscopy & Microanalysis Research Facility (AMMRF) at the Australian Centre for Microscopy & Microanalysis, The University of Sydney. This work was supported by a University of Sydney Fellowship and FABLS funding. L.D. thanks the NSF for financial support (Grant CMMI-0609077).

REFERENCES

- (1) Pazos-Perez, N.; Baranov, D.; Irsen, S.; Hilgendorff, M.; Liz-Marzan, L. M.; Giersig, M. *Langmuir* **2008**, *24* (17), 9855–9860.
- (2) Tang, Z. Y.; Kotov, N. A.; Giersig, M. *Science* **2002**, *297* (5579), 237–240.
- (3) Huang, Y.; Duan, X. F.; Wei, Q. Q.; Lieber, C. M. *Science* **2001**, *291* (5504), 630–633.
- (4) Whitesides, G. M.; Mathias, J. P.; Seto, C. T. *Science* **1991**, *254* (5036), 1312–1319.
- (5) Alivisatos, A. P. *Science* **1996**, *271* (5251), 933–937.
- (6) Alivisatos, A. P. *Science* **2000**, *289* (5480), 736–737.
- (7) Wu, Z. G.; Grossman, J. C. *Nano Lett.* **2008**, *8* (9), 2697–2705.
- (8) Yang, W. R.; Moghaddam, M.; Taylor, S.; Bojarski, B.; Wiecek, L.; Herrmann, J.; McCall, M. *Chem. Phys. Lett.* **2007**, *443* (4–6), 169–172.
- (9) Peng, X. H.; Chen, J. Y.; Misewich, J. A.; Wong, S. S. *Chem. Soc. Rev.* **2009**, *38* (4), 1076–1098.
- (10) Eder, D. *Chem. Rev.* **2010**, *110* (3), 1348–1385.
- (11) Nie, Z.; Petukhova, A.; Kumacheva, E. *Nat. Nanotechnol.* **2010**, *5* (1), 15–25.
- (12) Correa-Duarte, M. A.; Perez-Juste, J.; Sanchez-Iglesias, A.; Giersig, M.; Liz-Marzan, L. M. *Angew. Chem., Int. Ed.* **2005**, *44* (28), 4375–4378.
- (13) Xia, Y. N.; Yang, P. D.; Sun, Y. G.; Wu, Y. Y.; Mayers, B.; Gates, B.; Yin, Y. D.; Kim, F.; Yan, Y. Q. *Adv. Mater.* **2003**, *15* (5), 353–389.
- (14) Murphy, C. J.; Jana, N. R. *Adv. Mater.* **2002**, *14* (1), 80–82.
- (15) Lu, X. M.; Yavuz, M. S.; Tuan, H. Y.; Korgel, B. A.; Xia, Y. N. *J. Am. Chem. Soc.* **2008**, *130* (28), 8900–+.
- (16) Wang, C.; Hu, Y. J.; Lieber, C. M.; Sun, S. H. *J. Am. Chem. Soc.* **2008**, *130* (28), 8902–.
- (17) Huo, Z. Y.; Tsung, C. K.; Huang, W. Y.; Zhang, X. F.; Yang, P. D. *Nano Lett.* **2008**, *8* (7), 2041–2044.
- (18) Halder, A.; Ravishanker, N. *Adv. Mater.* **2007**, *19* (14), 1854–+.
- (19) Jiang, D. E.; Nobusada, K.; Luo, W. D.; Whetten, R. L. *ACS Nano* **2009**, *3* (8), 2351–2357.
- (20) Wang, C.; Sun, S. H. *Chem.—Asian J.* **2009**, *4* (7), 1028–1034.
- (21) Cademartiri, L.; Ozin, G. A. *Adv. Mater.* **2009**, *21* (9), 1013–1020.
- (22) Feng, H. J.; Yang, Y. M.; You, Y. M.; Li, G. P.; Guo, J.; Yu, T.; Shen, Z. X.; Wu, T.; Xing, B. G. *Chem. Commun.* **2009**, *15*, 1984–1986.
- (23) Kundu, P.; Halder, A.; Viswanath, B.; Kundu, D.; Ramanath, G.; Ravishanker, N. *J. Am. Chem. Soc.* **2010**, *132* (1), 20–.
- (24) Roldan, A.; Ricart, J. M.; Illas, F. *Mol. Simul.* **2009**, *35* (12–13), 1051–1056.
- (25) Kovtyukhova, N. I.; Mallouk, T. E. *Chem.—Eur. J.* **2002**, *8* (19), 4355–4363.
- (26) Carregal-Romero, S.; Buurma, N. J.; Perez-Juste, J.; Liz-Marzan, L. M.; Hervas, P. *Chem. Mater.* **2010**, *22* (10), 3051–3059.
- (27) Daw, M. S.; Baskes, M. I. *Phys. Rev. Lett.* **1983**, *50* (17), 1285–1288.
- (28) Daw, M. S.; Baskes, M. I. *Phys. Rev. B* **1984**, *29* (12), 6443–6453.
- (29) Brenner, D. W.; Shenderova, O. A.; Harrison, J. A.; Stuart, S. J.; Ni, B.; Sinnott, S. B. *J. Phys.: Condens. Matter* **2002**, *14* (4), 783–802.
- (30) Luedtke, W. D.; Landman, U. *Phys. Rev. Lett.* **1999**, *82* (19), 3835–3838.
- (31) Cleveland, C. L.; Luedtke, W. D.; Landman, U. *Phys. Rev. B* **1999**, *60* (7), 5065–5077.

- (32) Rodriguez-Lorenzo, L.; Aldeanueva-Potel, P.; Alvarez-Puebla, R. A.; Liz-Marzan, L. M.; de Abajo, F. J. G. *XXII Int. Conf. Raman Spectrosc.* **2010**, 1267, 927–927. 1294.
- (33) Alvarez-Puebla, R. A.; Liz-Marzan, L. M. *Energy Environ. Sci.* **2010**, 3 (8), 1011–1017.
- (34) Sanchez-Iglesias, A.; Grzelczak, M.; Perez-Juste, J.; Liz-Marzan, L. M. *Angew. Chem., Int. Ed.* **2010**, 49 (51), 9985–9989.
- (35) Juarez, B. H.; Klinke, C.; Kornowski, A.; Weller, H. *Nano Lett.* **2007**, 7 (12), 3564–3568.
- (36) Sanchez-Iglesias, A.; Grzelczak, M.; Rodriguez-Gonzalez, B.; Alvarez-Puebla, R. A.; Liz-Marzan, L. M.; Kotov, N. A. *Langmuir* **2009**, 25 (19), 11431–11435.
- (37) Lu, W.; Lieber, C. M. *Nat. Mater.* **2007**, 6 (11), 841–850.
- (38) Lu, W.; Xie, P.; Lieber, C. M. *IEEE Trans. Electron Devices* **2008**, 55 (11), 2859–2876.
- (39) Xia, Y.; Whitesides, G. M. *Angew. Chem., Int. Ed.* **1998**, 37, 551–575.
- (40) Aizenberg, J.; Black, A. J.; Whitesides, G. M. *Nature* **1999**, 398, 495–498.
- (41) Qu, L. T.; Du, F.; Dai, L. M. *Nano Lett.* **2008**, 8 (9), 2682–2687.
- (42) Dai, L. M.; Mau, A. W. H. *Adv. Mater.* **2001**, 13 (12–13), 899–.
- (43) Park, S. I.; Xiong, Y. J.; Kim, R. H.; Elvikis, P.; Meitl, M.; Kim, D. H.; Wu, J.; Yoon, J.; Yu, C. J.; Liu, Z. J.; Huang, Y. G.; Hwang, K.; Ferreira, P.; Li, X. L.; Choquette, K.; Rogers, J. A. *Science* **2009**, 325 (5943), 977–981.
- (44) Qu, L. T.; Peng, Q.; Dai, L. M.; Spinks, G. M.; Wallace, G. G.; Baughman, R. H. *MRS Bull.* **2008**, 33 (3), 215–224.
- (45) Pacifico, J.; van Leeuwen, Y. M.; Spuch-Calvar, M.; Sanchez-Iglesias, A.; Rodriguez-Lorenzo, L.; Perez-Juste, J.; Pastoriza-Santos, I.; Liz-Marzan, L. M. *Nanotechnology* **2009**, 20 (9), 095708.
- (46) Miranda, D.; Sencadas, V.; Sanchez-Iglesias, A.; Pastoriza-Santos, I.; Liz-Marzan, L. M.; Ribelles, J. L. G.; Lanceros-Mendez, S. *J. Nanosci. Nanotechnol.* **2009**, 9 (5), 2910–2916.
- (47) Das, R. N.; Lin, H. T.; Lauffer, J. M.; Markovich, V. R. *Circuit World* **2011**, 37 (1), 38–45.